RESEARCH ARTICLE

Identification of biomarkers associated with the development of hepatocellular carcinoma in CuZn superoxide dismutase deficient mice

Sailaja Elchuri[1], Mohammed Naeemuddin[1], Orr Sharpe[2], William H. Robinson[2, 3] and Ting-Ting Huang[1, 3]

[1] Department of Neurology and Neurological Sciences, Stanford University, Stanford, CA, USA
[2] Department of Medicine, Division of Immunology and Rheumatology, Stanford University, Stanford, CA, USA
[3] GRECC, VA Palo Alto Health Care System, Palo Alto, CA, USA

To identify biomarkers associated with the development of hepatocellular carcinoma (HCC) in CuZn superoxide dismutase (CuZnSOD, *Sod1*) deficient mice, 2-DE followed by MS analysis was carried out with liver samples obtained from 18-month-old *Sod1*−/− and +/+ mice. The intracellular Ca binding protein, regucalcin (RGN), showed a divergent alteration in *Sod1*−/− samples. Whereas elevated RGN levels were observed in −/− samples with no obvious neoplastic changes, marked reduction in RGN was observed in −/− samples with fully developed HCC. GST mu1 (GSTM1), on the other hand, showed a significant increase only in the neoplastic regions obtained from *Sod1*−/− livers. No change in GSTM1 was observed in the surrounding normal tissues. Marked reduction was observed in two intracellular lipid transporters, fatty acid binding protein 1 (FABP1) and major urinary protein 11 and 8 (MUP 11&8), in *Sod1*−/− samples. Analysis of additional samples at 18–22 months of age showed a three-fold increase in enolase activities in *Sod1*−/− livers. Consistent with previous findings, carbonic anhydrase 3 (CAIII) levels were significantly reduced in *Sod1*−/− samples, and immunohistochemical analysis revealed that the reduction was not homogenous throughout the lobular structure in the liver.

Received: December 13, 2006
Revised: March 9, 2007
Accepted: March 12, 2007

Keywords:
CuZn superoxide dismutase / GST mu1 / Hepatocellular carcinoma / Regucalcin / Senescence marker protein 30

1 Introduction

Hepatocellular carcinoma (HCC) is the major type of primary liver tumor and is one of the most common cancers worldwide [1, 2]. The disease has a very poor prognosis with greater than 50% of the patients dying within 1 year and only 2–6% surviving up to 5-year after diagnosis [3]. HCC does not respond well to surgery or chemotherapy and often requires a radical approach such as liver transplantation to prolong the survival of the patients. Therefore, the best approach in managing HCC is prevention. Consequently, identification of reliable serum and tissue markers for screening and monitoring of patients at high risk for developing HCC may lead to earlier intervention and better prognosis.

Hepatitis B virus (HBV) and hepatitis C virus (HCV) infections are the two major etiologies of HCC, and HBV and HCV infections have been shown to increase ROS production in patients [4]. Several clinical studies have also showed a causal relationship between HCC and low levels of superoxide dismutase (SOD) [5–8]. In our investigation of the

Correspondence: Dr. Ting-Ting Huang, 3801 Miranda Ave. Bldg 100, D3-101, Mail Stop 154-I, Palo Alto, CA 94304, USA
E-mail: tthuang@stanford.edu
Fax: +1-650-849-0457

Abbreviations: CAIII, carbonic anhydrase 3; **CuZnSOD,** CuZn superoxide dismutase; **FABP1,** fatty acid binding protein 1; **GSTM1,** GST mu1; **HCC,** hepatocellular carcinoma; **IHC,** immunohistochemistry; **MUP 11&8,** major urinary protein 11 and 8; **RGN,** regucalcin; **SMP30,** senescence marker protein 30

long-term effects of CuZn superoxide dismutase (CuZn-SOD) deficiency in mutant animals, we observed the development of HCC in B6-*Sod1* (gene designation for CuZn-SOD)−/− mice by 21 months of age [9]. In addition, liver-specific deletion of the transcription factor *Nrf1*, which mediates activation of oxidative stress response genes, leads to the development of HCC in adult mutant mice [10]. Taken together, the observations suggest that increased oxidative stress is a common factor in HCC development, and that studies on the hepatocarcinogenesis in *Sod1*−/− mice may provide important insights into the oxidative stress-mediated disease mechanism. As a first step to determine proteomic changes occurring in the oxidative stress-associated HCC development and to identify informative protein markers corresponding to the progression of hepatocarcinogenesis, we carried out 2-D/MS analysis on *Sod1*−/− and age-matched +/+ controls followed by immunochemical detection and transcriptional analysis of several proteins identified in this study.

2 Materials and methods

2.1 Sample preparation

All mice were housed in microisolators in the animal facility at the VA Palo Alto Health Care System. The mice were fed Harlan Teklad Global Rodent Diet 2019 (19% protein, 9% fat) from weaning till 2 months of age, and then switched permanently to a low fat diet (5% fat, Teklad Global Rodent Diet 2018). The mice were maintained on a 12 h light/dark cycle, at a constant temperature between 20 and 22°C, and given food and water *ad libitum*. Mice were checked daily by animal care personnel. All animal handling procedures were carried out according to the protocol approved by the Subcommittee on Animal Studies at the VA Palo Alto Health Care System. Liver samples were obtained from 3 to 6 and 18 to 22-month-old *Sod1*^{tm2}Cje +/+ and −/− mice on B6 background as previously described [9]. Liver samples from three *Sod1*+/+ and four *Sod1*−/− male mice at 18 months of age were used for 2-D/MS analysis. Three of the four *Sod1*−/− liver samples used for 2-D/MS analysis had fully developed HCC at the time of tissue collection; therefore, tumor tissues (*Sod1*−/− tumor) and the surrounding normal tissues (*Sod1*−/− non-tumor) from these three mice were analyzed separately. All +/+ control samples had normal histopathology. All of the samples used for 2-D/MS analysis were included in the 18–22-month-old group in the subsequent confirmation analyses by Western blotting, enzyme assay, and real time RT-PCR. Whenever possible, the same set of samples was used for all of the confirmational assays to track changes between histopathology status, protein levels, and message levels. Livers were homogenized in three volumes (w/v = 1:3) of lysis buffer containing 50 mM Tris-HCl pH 8.0, 0.6 mM $MnCl_2$, 2 mM citric acid, and the complete protease inhibitor cocktail (Roche, Indianapolis, IN, USA) and freeze–thawed three times between liquid nitrogen and room temperature water to disrupt the mitochondrial membrane. Tissue lysates were centrifuged at 10 000 × *g* at 4°C for 10 min and the supernatants were removed for the determination of protein concentration (BCA protein assay, Pierce, Rockford, IL) and aliquoted for storage at −80°C.

2.2 2-DE

2-DE was performed according to the procedure of Lanne *et al.* [11]. Briefly, proteins (200 μg) were precipitated from tissue lysates by 100% ice-cold acetone and dissolved in 150 μL of IEF buffer (8 M urea, 20 mM DTT, 2.0% w/v Chaps, 0.2% Biolytes, 2 M thiourea, and bromophenol blue). Protein concentration was determined again by Bradford method before loading. For the first-dimension electrophoresis, 150 μL (at 1 μg/μL) of sample solution was applied to an 11 cm Ready-Strip IPG strip, pH 3–10 (BioRad, Hercules, CA). Each sample was also separated with narrow range IPG strips (pH 4–7 and 7–10) for better sensitivity and resolution. The strips were soaked in the sample solution for 1 h to allow uptake of the proteins, then actively rehydrated in the Protean IEF cell (BioRad) for 12 h at 50 V. IEF was performed at the following voltage for 1 h each: 100, 200, 500, 1000; then accelerated to 8000 V in 30 min using a linear gradient and continued at 8000 V for 10 h. All the processes above were carried out at 22°C. The focused IEF strips were stored at −80°C until second-dimension electrophoresis was performed.

For second-dimension electrophoresis, thawed IPG strips were equilibrated for 15 min in 50 mM Tris-HCl pH 8.8, containing 6 M urea, 1% w/v SDS, 30% v/v glycerol, and 65 mM DTT, and re-equilibrated for 15 min in the same buffer containing 260 mM iodacetamide in place of DTT. Precast Criterion Tris-HCl gels (4–20% linear gradient, BioRad) were used to perform second-dimension electrophoresis. Protein standards were run along side the sample at 200 V for 60 min. After electrophoresis, the gels were washed in distilled water, stained in CBB for 1 h (Gelcode blue, Pierce), and destained overnight.

2.3 2-D gel analysis

The 2-D gel images were captured with a CCD camera (1280 × 960 pixels) using identical aperture setting and exposure time, and the spot intensities were analyzed using the PD Quest 2-D analysis software (version 8.0.1, BioRad). The intensity of each protein spot was assigned a value in PPM after normalization to total intensity of spots in the gel to eliminate differences in protein loading. The *Sod1*+/+, *Sod1*−/− tumor, and *Sod1*−/− non-tumor (the surrounding normal tissues) were analyzed as three different groups. Automatic spot matching function was used to match all the spots across all samples first; visual inspection was then carried out to make sure that spots were matched correctly. The intensity of certain unmatched spots, which may be present in one group of samples, but not in the others, was obtained

manually. The intensity value of missing spots was left blank, and the statistical analysis for those spots was not carried out. Instead, the spots were noted as absence in the dataset. Significant changes in spot intensity, as a function of protein expression, were calculated using Student's *t*-test between different groups.

2.4 MS analysis

Protein spots were cut out with a clean large-orifice pipette tip. To be certain of the protein identities, the same spots were usually picked from multiple gels from both +/+ and −/− samples whenever possible. Based on the molecular weight, p*I*, and the complete absence of the protein spot in all of the *Sod1*−/− gels (Fig. 1), the putative CuZnSOD spot was picked from all three *Sod1*+/+ pH 3–10 gels and from one *Sod1*+/+ pH 4–7 gel. Based on 2-D/Western blot results, the spot corresponding to actin was picked from one *Sod1*+/+ and one *Sod1*−/− gel. Gel spots were treated with 50% ACN in 10 mM ammonium bicarbonate (ABC) to remove the stain from the proteins, and with 100% ACN to dry the gel pieces. The dried gel pieces were rehydrated with 10% ACN in 10 mM ABC containing 0.1 mg trypsin *per* sample, incubated overnight at 37°C, and the resulting peptides were recovered with 60% ACN with 0.1% trifluoroacetate.

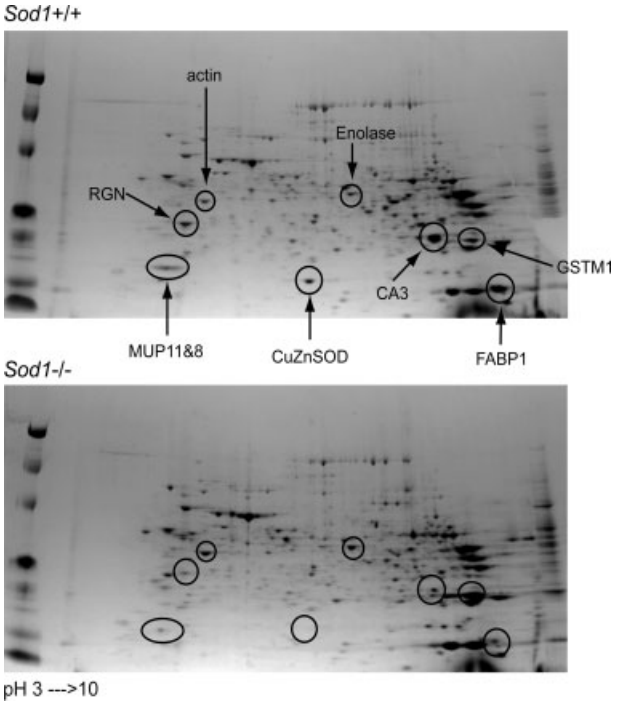

Figure 1. Comparison of 2-D gel patterns between *Sod1*+/+ and −/− liver samples. Representative gels (pH 3–10) generated from 18-month-old +/+ (top panel) and −/− (bottom panel) mice are shown. Protein spots corresponding to actin and the seven proteins listed in Table 1 are labeled.

The tryptic peptides were resolved by RP chromatography followed by MS/MS analysis as described in ref. [12]. The MS data were compared to simulated proteolysis and CID of the proteins in the NR-NCBI database using the Pep-Miner software (IBM, Haifa Research Lab) [12]. All MS analyses and protein digestions were carried out at the Smoler Proteomics Center, Technion, Haifa, Israel.

2.5 Immunodetections

1-D Western blot analyses of regucalcin (RGN), fatty acid binding protein 1 (FABP1), and actin were performed as previously described [9]. The primary antibodies against RGN (Clone Regucalcin M, Cell Sciences, Canton, MA), FABP1 (AF 1565, R&D Systems, Minneapolis, MN), and actin (A 5441, Sigma, St. Louis, MO) were used at 1:250, 1:1000, and 1:500 dilution, respectively. HRP-conjugated secondary antibodies were used at 1:4000 dilution. Actin was used as a loading control and all signal intensities were normalized to that of actin. To positively identify the protein spot for actin in 2-D gels, one pH 3–7 gel each from a +/+ and a −/− sample was transferred to NC filter and subjected to Western blot analysis after second-dimension electrophoresis. The Western blot analysis was carried out as previously described [9].

Immunohistochemical (IHC) analyses of carbonic anhydrase III (CAIII) were carried out on paraffin embedded liver sections from *Sod1*+/+ and −/− mice as described previously [9]. Primary antibody (PA-4010, Spectral Diagnostics, Toronto, Canada) and secondary antibody (SC2768, Santa Cruz Biotechnology) were used at 1:200 and 1:1000, respectively.

2.6 Enolase assay

Enolase activities were determined by monitoring the formation of 2-phosphoglyceric acid (2-PGA) from phosphoenol pyruvate (PEP) at 240 nm according to Pal-Bhowmick *et al.* [13]. The enzyme activity was calculated using ε_{240} nm = 1400/M/cm.

2.7 Quantification of mRNA by real time PCR

Total RNA from approximately 20 mg liver tissue was extracted and purified using TRIzol® reagent (Invitrogen, Carlsbad, CA) and RNeasy column (Qiagen, Valencia, CA). RNAs were quantified with a spectrophotometer (Beckman Coulter, Fullerton, CA). After DNase I digestion (amplification grade, 18068-0158, Invitrogen), 2 μg of total RNA was reverse-transcribed by Superscript II reverse transcriptase (Invitrogen) according to the manufacturer's protocol using random oligo-d(T) as primers. Real time PCR analysis was carried out on an ABI Prism 7900HT system (Applied Biosystems, Foster City, CA). PCR conditions were 95°C for 10 min followed by 40 cycles of 95°C for 15 s and 60°C for 1 min. Each reaction contained cDNA from 10 ng of RNA,

800 nM of each primer, and SYBR® Green QPCR Master Mix (Stratagene, La Jolla, CA) in a total volume of 6 μL. Primers were designed according to the guidelines in Primer Express (Applied Biosystems) software and are listed in Supporting Information Table 1. All samples were analyzed in triplicates and were quantified using a standard curve. Standards were generated by a serial dilution of cDNAs pooled from *Sod1*+/+ and −/− samples. The level of each mRNA was normalized to that of ubiquitin and expressed as fold change from that of age-matched controls.

2.8 Statistical analysis

Normalized signal intensities from Western blots were analyzed by Student's *t*-test using Prism 4 (GraphPad, San Diego, CA) and expressed as percentage of age-matched controls. Enolase activities and quantitative RT-PCR data were also analyzed by Student's *t*-test. Since a subset of *Sod1*−/− mice in the 18–22 months group have already developed HCC at the time of tissue collection, all data analyses for this group were carried out with tumor and non-tumor samples as two separate groups first. If there was a distinctive difference between these two, they were compared separately to +/+ controls (see notations in table and figure legends). On the other hand, if there was no discernable difference between the tumor and non-tumor group, the data were combined and compared to that of +/+ controls. Likewise, within the tumor-bearing group, results from tumor tissues and the surrounding normal tissues were analyzed separately to know if there was a difference between them.

3 Results

3.1 2D/MS comparison

Sod1−/− mice on B6 background develop HCC by 21 months of age [9], and a high percentage of mice already have fully developed HCC by 18 months. Therefore, we chose 18 months as the age for our proteomic analysis. A total of 50 spots were picked from 2-D gels for MS analysis, and a total of 70 proteins were identified by a minimum of 3 peptides each from the 50 gel spots. MS analysis confirmed the identity of CuZnSOD and actin in the corresponding gel spots (data not shown). Proteins that showed a consistent difference between +/+ and −/− samples are listed in Table 1 and the normalized signal intensities presented in Fig. 2. The peptide sequences identified by MS analysis are also listed in Supporting Information Table 2. The magnitude of difference between +/+ and −/− was the largest in major urinary protein 11 and 8 (MUP 11&8), followed by CAIII, RGN, and FABP1 (Figs. 2a and b). There was no significant difference between tumor and the surrounding normal tissue in −/− samples within this group of proteins. On the other hand, a significant difference in GST mu1 (GSTM1)

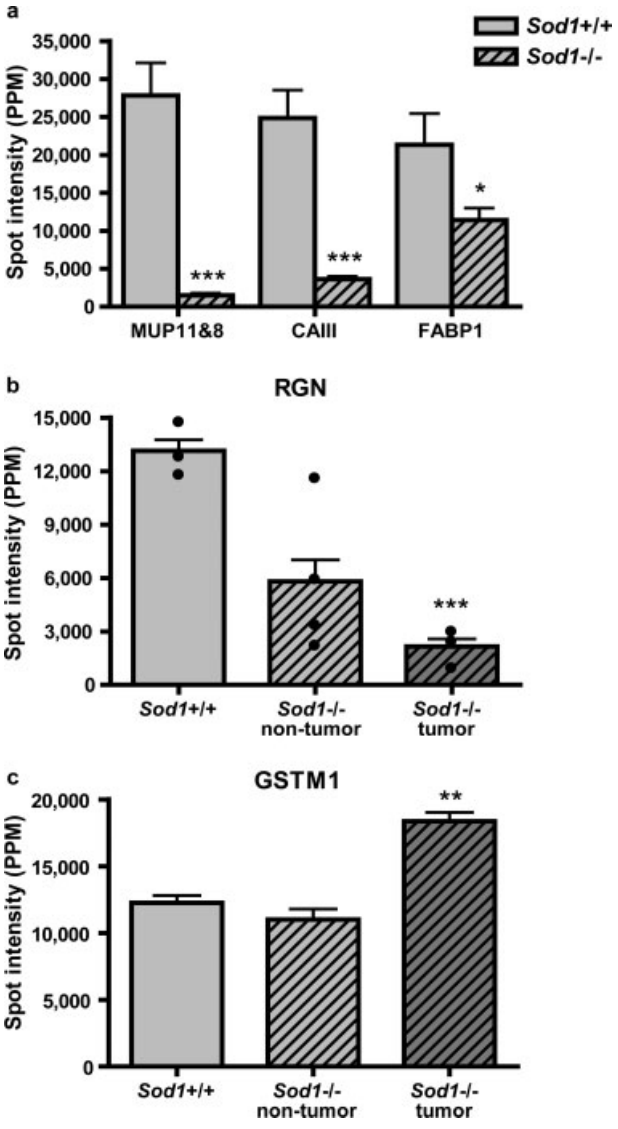

Figure 2. Abundance of proteins that showed a consistent difference between *Sod1*+/+ and −/− samples. (a) MUP11&8, CAIII, and FABP1. Significant reduction of these three proteins was observed in all *Sod1*−/− samples regardless of the histopathology status. (b) RGN. The nontumor samples (*Sod1*−/− non-tumor) have a wide distribution in RGN levels due to the differences in the histopathology status of the mice from which these samples were collected. To more clearly illustrate the disparity, spot intensity of each individual data point (●) is plotted along the bar graph. (c) GSTM1. Significant increase in GSTM1 level was observed in the liver tumors retrieved from *Sod1*−/− samples (*Sod1*−/− tumor). On the other hand, no significant change in GSTM1 level was observed in the normal surrounding tissues in *Sod1*−/− samples (*Sod1*−/− non-tumor). All data represent mean ± SEM. Sample sizes are the same as that specified in Table 1. *$p<0.05$; **$p<0.01$; ***$p<0.001$.

levels was observed between the tumor and the surrounding normal tissues in *Sod1*−/− livers that developed HCC. Thus, a 50% increase in GSTM1 was only observed in the

Table 1. Changes in 2-D gel profiles in *Sod1*−/− livers

Protein ID	p*I*/MW (kDa)	Number of peptides matched	Percent coverage by matched peptides (%)	Score[a)]	Number of gel spots analyzed by MS	Change in *Sod1*−/− (% +/+ level)[b)]		
						Non-tumor	Tumor	Total
CuZnSOD	6.02/15.9	10	51	87.4	4	Not present	Not present	Not present
CAIII	6.89/29.3	14	44	89.1	3	17.8%**	10.3%*	14.6%***
Enolase	6.37/47.1	31	37	90.5	2	146%	139%	143%
FABP1	8.59/14.2	13	54	89.4	3	76.9%	22.2%*	53.5%*
GSTM1	8.14/25.8	23	43	88.7	3	89.8%	149.6%**[c)]	115.5%
MUP 11&8	4.85/17.6	20	55	90.5	3	9.1%**	0.6%**	5.4%***
RGN	5.16/33.4	25	51	91.6	5	44.1%*[d)]	16.3%***	32.2%**

a) Each peptide received a score for the matching to the candidate protein. A score of greater than 60 is considered a good match. The average score of all the peptides sequenced for each protein is presented.

b) The signal intensity of each spot was quantified by the PDQuest 2-D analysis software and normalized to that of total intensity of each gel. Statistical analyses were carried out separately for the non-tumor (normal surrounding tissue, $n = 4$) and tumor ($n = 3$) *Sod1*−/− samples. Comparisons between *Sod1*+/+ and data from all the *Sod1*−/− samples (total; non-tumor plus tumor *Sod1*−/− samples) are also presented.

c) GSTM1 levels were not significantly altered in the non-tumor *Sod1*−/− samples, but were significantly increased (149.6%, $p = 0.0077$) in the corresponding tumor samples.

d) Among the four non-tumor *Sod1*−/− samples, three were collected from tumor-bearing *Sod1*−/− mice as the normal surrounding tissues. Similar to their tumor counterparts, the RGN level in these three samples are substantially lower than that of *Sod1*+/+ samples. On the other hand, the non-tumor *Sod1*−/− sample collected form a non-tumor-bearing mouse has an RGN level closer to that of *Sod1*+/+ samples (see data point distribution in *Sod1*−/−non-tumor in Fig. 2b). Consequently, the average RGN level from these four non-tumor samples showed a significant deviation from that of *Sod1*+/+ controls.
*$p<0.05$; **$p<0.01$; ***, $p<0.001$.

neoplastic regions, and no significant difference in GSTM1 was detected between +/+ controls and −/− samples with normal histopathology (Fig. 2c).

3.2 Western blotting and immunohistochemical confirmation of 2-D gel results

To confirm the 2-D gel results and to know age-related changes in a subset of proteins, Western blot analysis was carried out with additional liver samples collected from 3 to 6 and 18–22-month-old mice. The two ages represent *Sod1*−/− mice that are relatively healthy with no overt abnormalities (3–6 months) and *Sod1*−/− mice that are near end-stage (18–22 months) with roughly 30% of them with well-established HCC [9]. Consistent with the 2-D gel results, FABP1 showed a 70 and 55% reduction in the −/− livers at 3–6 months and 18–22 months, respectively (Fig. 3a), regardless of the histopathology status. The data suggest that reduction in FABP1 may be directly related to CuZnSOD deficiency, and not as a consequence of hepatocarcinogenesis. RGN also showed a 56% reduction in the −/− livers at 3–6 months, but the difference was not statistically significant (Fig. 3b). In 2-D gel analysis, we observed a large deviation of RGN level between the *Sod1*−/− sample collected from a non-tumor-bearing mouse (normal level of RGN) and that in the *Sod1*−/− samples collected from tumor-bearing mice (low levels of RGN) in the *Sod1*−/− non-tumor group (Fig. 2b). The difference may be due to the histopathological state of the mice from which the samples were collected. To resolve this discrepancy, we collected more samples from non-tumor-bearing *Sod1*−/− mice and carried out Western blot to see if the relatively normal level of RGN observed in the non-tumor-bearing mouse can be reproduced in a larger set of samples. Consistent with the 2-D gel results, *Sod1*−/− samples with normal histopathology (18–22N) showed an average of 70% increase in RGN levels (Fig. 3b). On the other hand, the 18–22-month-old samples with obvious HCC development (18–22T) showed a 50% reduction by Western blot analysis. The divergence in RGN levels between tumor-bearing and non-tumor-bearing *Sod1*−/− samples is noteworthy and the difference is likely related to the development of hepatocarcinogenesis. Among the −/− liver samples with reduced RGN levels, there was no discernable difference in RGN between the tumor and the surrounding normal tissue (data not shown).

We showed the reduction of CAIII in *Sod1*−/− livers previously by Western blot analysis [9], and the results were confirmed by 2-D/MS analysis in this study (Fig. 2a). To further identify the reduction of CAIII at the cellular level, IHC analysis was carried out. The results showed that reduction of CAIII was not homogenous across all regions (Fig. 4). Although the majority of −/− cells had very low level, a small number of cells actually had higher than normal levels of CAIII. Nuclear localization of CAIII was also observed in a subset of cells in *Sod1*−/− sections.

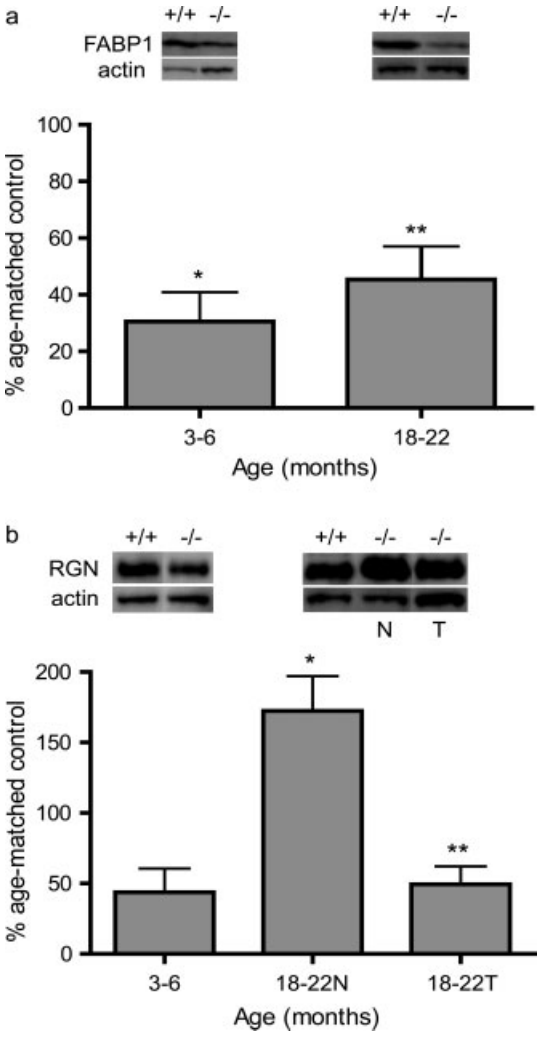

Figure 3. Quantitative Western blot analysis of FABP1 and RGN. (a) Significant reduction in FABP1 levels was observed in the liver of 3–6 and 18–22-month-old *Sod1*−/− mice regardless of histopathology status. (b) Significant increase and decrease in RGN levels was observed in 18–22N (collected from mice with normal histopathology) and 18–22T (represent liver tumors collected from tumor-bearing mice) *Sod1*−/− liver samples, respectively. Increased levels of RGN were associated with mice with a normal histopathology, while decreased levels of RGN were associated with the development of HCC in *Sod1*−/− mice. Sample size: 3–6 months, $n = 4$ each; 18–22 months, $n = 6$ for +/+ and $n = 9$ for −/− samples. For RGN analysis, the 18–22-month-old *Sod1*−/− samples were further divided into normal (N, $n = 6$) and tumor (T, $n = 3$) group based on histopathology data. Protein levels form *Sod1*−/− samples are presented as % age-matched control. $*p<0.02$; $**p<0.002$.

3.3 Enolase activities are increased in 18–22-month-old *Sod1*−/− livers

Increased dependence on glycolysis is common in tumor tissues [14]. To determine if enzymes in the glycolysis pathway were upregulated in *Sod1*−/−, liver samples from 3–6 and 18–22-month-old mice were used for a direct measurement of enolase activities. No difference in enolase activities was observed between *Sod1*+/+ and −/− at 3–6 months of age. However, by the time the mice reached 18–22-month-old, there was a three-fold difference between +/+ and −/− samples (Fig. 5) regardless of liver pathology. Among the +/+ samples, there was a 50% reduction from 3 to 6 months to 18–22 months. In contrast, a two-fold increase from 3–

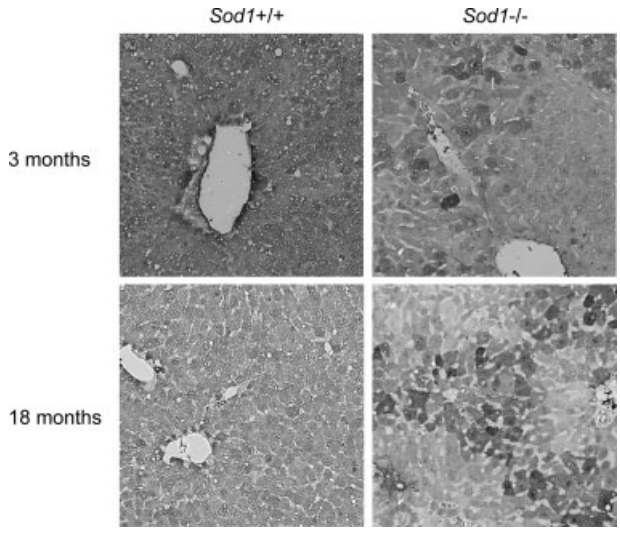

Figure 4. Immunohistochemical analysis of CAIII. Representative liver sections from 3- and 18-month-old *Sod1*+/+ and −/− mice are shown. A mosaic staining pattern is commonly observed in *Sod1*−/− samples, suggesting a heterogeneous expression of CAIII among different hepatocytes. Positive staining signals were also observed in the nucleus in a subset of cells. Five each +/+ and −/− samples were examined.

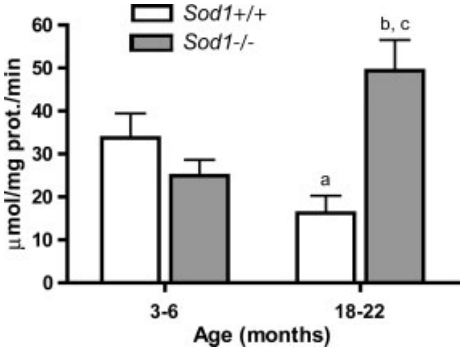

Figure 5. Enolase activities. A three-fold increase in enolase activities was observed in 18–22-month-old *Sod1*−/− samples. Sample size: 3–6 months, $n = 4$ each; 18–22 months, $n = 6$ for +/+ and $n = 9$ for −/− samples. No discernable difference in enolase activities was observed between tumor and non-tumor *Sod1*−/− samples in the 18–22 months group. Therefore, combined data are reported here. (a) Significantly different from 3–6 months *Sod1*+/+ ($p = 0.007$); (b) significantly different from 3 to 6 months *Sod1*−/− ($p = 0.018$); (c) significantly different from 18–22 months *Sod1*+/+ ($p = 0.0005$).

6 months to 18–22 months was observed in −/− samples. The data suggest a possible shift to glycolysis as *Sod1*−/− mice age.

3.4 qRT-PCR analysis suggests transcriptional and post-transcriptional regulation of protein levels

To determine if the observed changes in 2-D analysis occurred at the transcriptional level, quantitative RT-PCR analyses were carried out on the proteins listed in Table 1. Consistent with our previous observation, message levels for CAIII (*Car3*) were already significantly reduced at 3–6 months (data not shown), and the reduction became more pronounced at 18–22 months in *Sod1*−/− samples (Fig. 6). All other proteins did not show a difference at the transcriptional level at 3–6 months of age (data not shown). However, by 18–22 months of age, *Sod1*−/− mice were showing a consistent decrease in the message levels in fatty acid binding protein 1 (*Fabp1*), regucalcin (*Rgn*), and major urinary protein 11&8 (*Mup11&8*) in the liver. On the other hand, no change in enolase (*Eno1)* and glutathione S-transferase mu1 (*Gstm1*) message levels was detected. There was no clear distinction in the message level between tumor-bearing and normal *Sod1*−/− samples. The concordant change between protein and message in CAIII, FABP1, and MUP 11&8 suggests a regulation at the transcriptional level. On the other hand, the lack of concordant change between protein and message in RGN and enolase suggests a posttranscriptional regulation of these two proteins in CuZnSOD deficient environment.

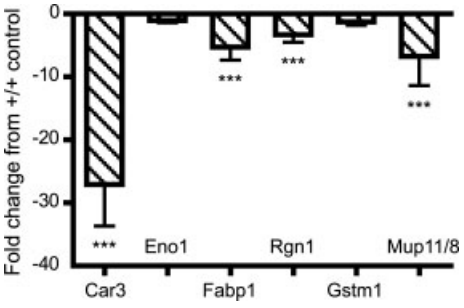

Figure 6. Quantitative RT-PCR analysis. Message levels in 18–22-month-old *Sod1*+/+ and −/− liver samples were quantified and normalized to that of ubiquitin in each sample. Sample size: $n = 6$ for +/+ and $n = 8$ for −/− samples. ***$p<0.001$. No discernable difference in message levels was observed among *Sod1*−/− samples with or without tumor. Therefore, the data were combined and compared with that of +/+ controls.

4 Discussion

To determine the effects of CuZnSOD deficiency on the proteomic changes in *Sod1*−/− livers and to identify informative protein markers that correlate with hepatocarcinogenesis, we carried out 2-D/MS analysis on *Sod1* mutant mice at 18 months of age, a stage when a subpopulation of *Sod1*−/− mice already have well-established hepatocarcinogenesis. Three of the four *Sod1*−/− mice used for 2-D/MS analysis have developed HCC at the time of tissue collection. This enabled us to compare between tumor and its surrounding normal tissue from the same mutant mouse.

Both RGN and GSTM1 showed important correlations with hepatocarcinogenesis. RGN levels were markedly reduced in −/− liver samples with well-established HCC, but elevated in −/− liver samples with no overt histopathological abnormalities (Table 1, Figs. 2b and 3b). The reduction in RGN was not limited to tumors; normal adjacent tissues also showed a similar level of reduction. Notably, reduction of RGN in clinical HCC samples has been demonstrated in two separate proteomic studies [15, 16], and substantial reduction in RGN expression has been shown in GST plascental form (GST-P) positive preneoplastic foci in a rat model of diethyl nitrosamine (DEN)/2-acetylaminofluorene (2-AAF)/partial hepatectomy (PH)-induced HCC [17]. Therefore, RGN level may be a useful biomarker for following the development of HCC in human population predisposed to the development of HCC and in mouse models of hepatocarcinogenesis. How does a change in RGN level relate to the pathogenesis of HCC? RGN is a Ca binding protein and is important for intracellular Ca homeostasis and in signaling pathways controlling glucose utilization and lipid production [18–20]. RGN is sensitive to oxidative modification and a more than two-fold increase in the carbonyl content has been reported in old mice [21]. RGN is also known as senescence marker protein 30 (SMP30) [22]. Overexpression of RGN in the rat hepatoma cell line H4-II-E was shown to suppress the expression of oncogenes c-myc, Haras, and c-src, and increase the expression of tumor suppressor genes p53 and Rb [23, 24]. Recent studies in hepatoma cell lines also showed growth suppression effects by RGN [25, 26]. Therefore, upregulation of RGN may provide the benefit of suppressing hepatocarcinogenesis in *Sod1*−/− mice, whereas reduced expression of RGN may have the opposite effect. A recent report showed that SMP30 functions as a gluconolactonase, which is involved in the *de novo* synthesis of ascorbic acid [27, 28]. Consequently, SMP30 knockout mice are severely vitamin C deficient, containing only 6–8% of the tissue and plasma vitamin C levels found in wild-type controls even though vitamin C is supplemented (55 mg/kg) in the mouse chow [27]. Furthermore, when SMP30 knockout mice are fed a vitamin C-deficient diet, they develop symptoms of scurvy [27]. It is possible that upregulation of RGN in *Sod1*−/− livers helps to increase the tissue level of vitamin C and thus, helps to alleviate the oxidative stress imposed by CuZnSOD deficiency. Upregulation of RGN in *Sod1*−/− livers may also lead to a better-regulated intracellular calcium homeostasis, reduced cell death, and suppression of oncogene expressions. These modulations then help to prevent the development of hepatocarcinogenesis. On the other hand, reduced RGN in *Sod1*−/− livers

would likely lead to vitamin C deficiency and further exacerbate the extent of oxidative stress. Reduced levels of RGN may also sensitize hepatocytes to apoptosis, enhance tumor-related gene expression, and ultimately, facilitate the development of hepatocarcinogenesis.

GSTM1 protein levels were only increased in the tumors of tumor-bearing *Sod1*−/− livers (Table 1, Figs. 1 and 2c), and no change in GSTM1 was detected in the adjacent normal tissues. This is reminiscent of the expression pattern of another GST isoform, GST-P, in preneoplastic foci in rat chemical hepatocarcinogenesis [29]. GSTM1 belongs to a large group of detoxifying proteins that inactivate reactive intermediates by conjugating glutathione (GSH) to the reactive intermediates [30]. Both constitutive and inducible expression of GSTM1 has been shown to be controlled by the transcription factor *Nrf2* [31]. Interestingly, GSTM1 was also shown to be transcriptionally upregulated by the Myb oncoprotein [32]. In addition, GSTM1 has been shown to inhibit MEK kinase 1 (MEKK1) activity and suppress MEKK1-medaited apoptosis [33]. Therefore, increased GSTM1 levels in tumor tissues may be a consequence of oncogenic induction, and increased GSTM1 may play a role in tumor survival.

Other proteins identified in this study did not show an association with hepatocarcinogenesis in *Sod1*−/−, and the changes were most likely a consequence of CuZnSOD deficiency. However, alteration in these proteins may eventually contribute to different aspects of hepatocarcinogenesis. These proteins include enolase, FABP1, MUP 11&8, and CAIII. Alterations of these proteins tend to occur earlier and in larger magnitude. Enolase activities were increased by three-fold in 18–22-month-old *Sod1*−/− mice (Fig. 5). Similarly, a recent proteomic study with HCV-associated HCC samples showed a positive correlation between α-enolase levels and the severity of the tumors [34]. Upregulation of enzymes in the glycolysis pathway is common in various types of tumors [14], and may reflect the metabolic shift in tumor cells in response to the hypoxic growth environment [35]. In addition to being part of the glycolysis pathway, enolase, and a number of other glycolytic enzymes have been localized in the nucleus [36] and shown to play a role in transcriptional regulation. Several studies have identified the Myc promoter-binding protein-1 (MBP-1), a transcriptional suppresser of Myc, as an alternative translation product of *Eno1* [36]. Since *Eno1* is upregulated by Myc overexpression [37], enolase-mediated transcriptional suppression of Myc likely serves as a negative feedback on Myc-induced glycolysis.

Consistent with our previous finding [9], total protein levels of CAIII was reduced in *Sod1*−/− livers due to transcriptional downregulation of *Car3* (Table 1, Figs. 2a and 6). However, IHC analysis revealed a mosaic expression pattern, with some cells expressing higher than control level and most cells totally devoid of CAIII in *Sod1*−/− lives (Fig. 4). The significance of CAIII reduction on hepatocarcinogenesis in *Sod1*−/− mice is not clear. CAIII null mutant mice have been generated, and no obvious phenotype has been attributed to CAIII deficiency [38]. However, expression of *Car3* in cells lacking the protein protects the cells from hydrogen peroxide-induced apoptosis [39]. Therefore, CAIII deficiency in *Sod1*−/− mice may further reduce cellular resistance to oxidative stress and amplify the deleterious effects of CuZn-SOD deficiency.

Reduced FABP1 levels were observed at as early as 3 months of age in *Sod1*−/− liver samples (Table 1, Figs. 2a and 3a). FABP1, also called L-FABP for its dominance in the liver, is a cytosolic protein and acts as intracellular transporter of fatty acids between membranes [40]. Deletion of FABP1 in mutant mice causes problem in branched-chain fatty acid metabolism [41]. A recent study showed the antioxidant function of FABP1, and increased expression of FABP1 in a liver cell line reduced cellular damage from hypoxia/reoxygenation [42]. Therefore, similar to CAIII deficiency, reduced FABP1 may contribute to a further increase in oxidative damage in *Sod1*−/− mice. Marked reduction of MUP 11&8 was consistently observed in *Sod1*−/− samples (Table 1, Figs. 1 and 2a), and the reduction was controlled at the transcriptional level (Fig. 6). MUP 11&8 belong to the lipocalin family and, similar to FABP1, are responsible for transporting small hydrophobic molecules such as lipids and volatile pheromones [43]. The concomitant reduction of FABP1 and MUP 11&8 suggests a dramatic change in intracellular lipid transport in *Sod1*−/− mice.

In summary, alterations in the levels or activities of several proteins were identified in the liver of *Sod1*−/− mice by 2-D/MS analysis. RGN and GSTM1 showed a distinctive correlation with hepatocarcinogenesis. Reduction of RGN was associated with the development of HCC, whereas increased RGN levels were associated with normal histopathology in *Sod1*−/− livers. On the other hand, increased levels of GSTM1 were only observed in the neoplastic region of tumor-bearing *Sod1*−/− livers. The difference in RGN levels is particularly important as it showed a clear divergence between tumor-bearing and non-tumor-bearing *Sod1*−/− samples. Further studies will be required to determine the mechanism controlling RGN levels in the CuZn-SOD deficient environment and how changes in RGN levels affect the development of HCC.

This work was supported by funding from the National Institutes of Health (AG24400), the Stanford Cancer Council, and the Digestive Disease Center at Stanford University. Mass spectrometry analysis was carried out at the Technion Smoler Proteomics Center, Israel.

5 References

[1] Murray, C. J., Lopez, A. D., *Lancet* 1997, *349*, 1436–1442.

[2] Levy, L., Renard, C. A., Wei, Y., Buendia, M. A., *Ann. N. Y. Acad. Sci.* 2002, *963*, 21–36.

[3] Hoofnagle, J. H., *Gastroenterology* 2004, *127*, S319–S323.

[4] Valgimigli, M., Valgimigli, L., Trere, D., Gaiani, S. *et al.*, *Free Radic. Res.* 2002, *36*, 939–948.

[5] Casaril, M., Corso, F., Bassi, A., Capra, F. *et al.*, *Int. J. Clin. Lab. Res.* 1994, *24*, 94–97.

[6] Huang, C., Wu, M., *Zhonghua Yi Xue Za Zhi* 1990, *70*, 138–139.

[7] Inagaki, T., Katoh, K., Takiya, S., Ikuta, K. *et al.*, *Gastroenterol. Jpn.* 1992, *27*, 382–389.

[8] Liaw, K. Y., Lee, P. H., Wu, F. C., Tsai, J. S., Lin-Shiau, S. Y., *Am. J. Gastroenterol.* 1997, *92*, 2260–2263.

[9] Elchuri, S., Oberley, T. D., Qi, W., Eisenstein, R. S. *et al.*, *Oncogene* 2005, *24*, 367–380.

[10] Xu, Z., Chen, L., Leung, L., Yen, T. S. *et al.*, *Proc. Natl. Acad. Sci. USA* 2005, *102*, 4120–4125.

[11] Lanne, B., Potthast, F., Hoglund, A., Brockenhuus von Lowenhielm, H. *et al.*, *Proteomics* 2001, *1*, 819–828.

[12] Beer, I., Barnea, E., Ziv, T., Admon, A., *Proteomics* 2004, *4*, 950–960.

[13] Pal-Bhowmick, I., Sadagopan, K., Vora, H. K., Sehgal, A. *et al.*, *Eur. J. Biochem.* 2004, *271*, 4845–4854.

[14] Altenberg, B., Greulich, K. O., *Genomics* 2004, *84*, 1014–1020.

[15] Kim, W., Oe Lim, S., Kim, J. S., Ryu, Y. H. *et al.*, *Clin. Cancer Res.* 2003, *9*, 5493–5500.

[16] Kim, J., Kim, S. H., Lee, S. U., Ha, G. H. *et al.*, *Electrophoresis* 2002, *23*, 4142–4156.

[17] Suzuki, S., Asamoto, M., Tsujimura, K., Shirai, T., *Carcinogenesis* 2004, *25*, 439–443.

[18] Yamaguchi, M., *Int. J. Mol. Med.* 2005, *15*, 371–389.

[19] Fujita, T., Shirasawa, T., Inoue, H., Kitamura, T., Maruyama, N., *J. Gastroenterol. Hepatol.* 1998, *13*, S124–S131.

[20] Nakashima, C., Yamaguchi, M., *J. Cell. Biochem.* 2006, *99*, 1582–1592.

[21] Chaudhuri, A. R., de Waal, E. M., Pierce, A., Van Remmen, H. *et al.*, *Mech. Ageing Dev.* 2006, *127*, 849–861.

[22] Fujita, T., *Biochem. Biophys. Res. Commun.* 1999, *254*, 1–4.

[23] Tsurusaki, Y., Yamaguchi, M., *J. Cell. Biochem.* 2003, *90*, 619–626.

[24] Tsurusaki, Y., Yamaguchi, M., *Int. J. Mol. Med.* 2004, *14*, 277–281.

[25] Yamaguchi, M., Daimon, Y., *J. Cell. Biochem.* 2005, *95*, 1169–1177.

[26] Yamaguchi, M., Kobayashi, M., Uchiyama, S., *J. Cell. Biochem.* 2005, *96*, 543–554.

[27] Kondo, Y., Inai, Y., Sato, Y., Handa, S. *et al.*, *Proc. Natl. Acad. Sci. USA* 2006, *103*, 5723–5728.

[28] Linster, C. L., Van Schaftingen, E., *FEBS J.* 2007, *274*, 1–22.

[29] Sato, K., Kitahara, A., Satoh, K., Ishikawa, T. *et al.*, *Gann* 1984, *75*, 199–202.

[30] Hayes, J. D., Flanagan, J. U., Jowsey, I. R., *Annu. Rev. Pharmacol. Toxicol.* 2005, *45*, 51–88.

[31] Chanas, S. A., Jiang, Q., McMahon, M., McWalter, G. K. *et al.*, *Biochem. J.* 2002, *365*, 405–416.

[32] Bartley, P. A., Keough, R. A., Lutwyche, J. K., Gonda, T. J., *Oncogene* 2003, *22*, 7570–7575.

[33] Ryoo, K., Huh, S. H., Lee, Y. H., Yoon, K. W. *et al.*, *J. Biol. Chem.* 2004, *279*, 43589–43594.

[34] Takashima, M., Kuramitsu, Y., Yokoyama, Y., Iizuka, N. *et al.*, *Proteomics* 2005, *5*, 1686–1692.

[35] Leo, C., Giaccia, A. J., Denko, N. C., *Semin. Radiat. Oncol.* 2004, *14*, 207–214.

[36] Kim, J. W., Dang, C. V., *Trends Biochem. Sci.* 2005, *30*, 142–150.

[37] Kim, J. W., Zeller, K. I., Wang, Y., Jegga, A. G. *et al.*, *Mol. Cell. Biol.* 2004, *24*, 5923–5936.

[38] Kim, G., Lee, T. H., Wetzel, P., Geers, C. *et al.*, *Mol. Cell. Biol.* 2004, *24*, 9942–9947.

[39] Raisanen, S. R., Lehenkari, P., Tasanen, M., Rahkila, P. *et al.*, *FASEB J.* 1999, *13*, 513–522.

[40] Martin, G. G., Danneberg, H., Kumar, L. S., Atshaves, B. P. *et al.*, *J. Biol. Chem.* 2003, *278*, 21429–21438.

[41] Atshaves, B. P., McIntosh, A. L., Payne, H. R., Mackie, J. *et al.*, *Am. J. Physiol. Cell Physiol.* 2005, *288*, C543–C558.

[42] Wang, G., Gong, Y., Anderson, J., Sun, D. *et al.*, *Hepatology* 2005, *42*, 871–879.

[43] Beynon, R. J., Hurst, J. L., *Biochem. Soc. Trans.* 2003, *31*, 142–146.

